INTERNATIONAL STANDARD

ISO 28902-2

First edition
2017-07

Air quality — Environmental meteorology —

Part 2: Ground-based remote sensing of wind by heterodyne pulsed Doppler lidar

Qualité de l'air — Météorologie de l'environnement —

Partie 2: Télédétection du vent par lidar Doppler pulsé hétérodyne basée sur le sol

Reference number
ISO 28902-2:2017(E)

ISO copyright office
Ch. de Blandonnet 8 • CP 401
CH-1214 Vernier, Geneva, Switzerland
Tel. +41 22 749 01 11
Fax +41 22 749 09 47
copyright@iso.org
www.iso.org

Contents

Page

Foreword ... **iv**

Introduction ... **v**

1 Scope ... **1**

2 Normative references ... **1**

3 Terms and definitions ... **1**

4 Fundamentals of heterodyne pulsed Doppler lidar ... **4**
4.1 Overview ... 4
4.2 Heterodyne detection ... 5
4.3 Spectral analysis ... 7
4.4 Target variables ... 10
4.5 Sources of noise and uncertainties ... 10
4.5.1 Local oscillator shot noise ... 10
4.5.2 Detector noise ... 11
4.5.3 Relative intensity noise (RIN) ... 11
4.5.4 Speckles ... 11
4.5.5 Laser frequency ... 11
4.6 Range assignment ... 11
4.7 Known limitations ... 11

5 System specifications and tests ... **12**
5.1 System specifications ... 12
5.1.1 Transmitter characteristics ... 12
5.1.2 Transmitter/receiver characteristics ... 13
5.1.3 Signal sampling parameters ... 13
5.1.4 Pointing system characteristics ... 14
5.2 Relationship between system characteristics and performance ... 15
5.2.1 Figure of merit ... 15
5.2.2 Time-bandwidth trade-offs ... 16
5.3 Precision and availability of measurements ... 17
5.3.1 Radial velocity measurement accuracy ... 17
5.3.2 Data availability ... 17
5.3.3 Maximum operational range ... 17
5.4 Testing procedures ... 18
5.4.1 General ... 18
5.4.2 Radial velocity measurement validation ... 18
5.4.3 Assessment of accuracy by intercomparison with other instrumentation ... 20
5.4.4 Maximum operational range validation ... 21

6 Measurement planning and installation instructions ... **23**
6.1 Site requirements ... 23
6.2 Limiting conditions for general operation ... 23
6.3 Maintenance and operational test ... 24
6.3.1 General ... 24
6.3.2 Maintenance ... 24
6.3.3 Operational test ... 24
6.3.4 Uncertainty ... 24

Annex A (informative) **Continuous-wave Doppler wind lidar** ... **26**

Annex B (informative) **Retrieval of the wind vector** ... **27**

Annex C (informative) **Applications** ... **32**

Annex D (informative) **Typical application ranges and corresponding requirements** ... **36**

Bibliography ... **38**

Foreword

ISO (the International Organization for Standardization) is a worldwide federation of national standards bodies (ISO member bodies). The work of preparing International Standards is normally carried out through ISO technical committees. Each member body interested in a subject for which a technical committee has been established has the right to be represented on that committee. International organizations, governmental and non-governmental, in liaison with ISO, also take part in the work. ISO collaborates closely with the International Electrotechnical Commission (IEC) on all matters of electrotechnical standardization.

The procedures used to develop this document and those intended for its further maintenance are described in the ISO/IEC Directives, Part 1. In particular the different approval criteria needed for the different types of ISO documents should be noted. This document was drafted in accordance with the editorial rules of the ISO/IEC Directives, Part 2 (see www.iso.org/directives).

Attention is drawn to the possibility that some of the elements of this document may be the subject of patent rights. ISO shall not be held responsible for identifying any or all such patent rights. Details of any patent rights identified during the development of the document will be in the Introduction and/or on the ISO list of patent declarations received (see www.iso.org/patents).

Any trade name used in this document is information given for the convenience of users and does not constitute an endorsement.

For an explanation on the voluntary nature of standards, the meaning of ISO specific terms and expressions related to conformity assessment, as well as information about ISO's adherence to the World Trade Organization (WTO) principles in the Technical Barriers to Trade (TBT) see the following URL: www.iso.org/iso/foreword.html.

This document was prepared by Technical Committee ISO/TC 146, *Air quality*, Subcommittee SC 5, *Meteorology*, and by the World Meteorological Organization (WMO) as a common ISO/WMO Standard under the Agreement on Working Arrangements signed between the WMO and ISO in 2008.

A list of all parts in the ISO 28902 series can be found on the ISO website.

Introduction

Lidars ("light detection and ranging"), standing for atmospheric lidars in the scope of this document have proven to be valuable systems for remote sensing of atmospheric pollutants, of various meteorological parameters such as clouds, aerosols, gases and (where Doppler technology is available) wind. The measurements can be carried out without direct contact and in any direction as electromagnetic radiation is used for sensing the targets. Lidar systems, therefore, supplement the conventional in-situ measurement technology. They are suited for a large number of applications that cannot be adequately performed by using in situ or point measurement methods.

There are several methods by which lidar can be used to measure atmospheric wind. The four most commonly used methods are pulsed and continuous wave coherent Doppler wind lidar, direct-detection Doppler wind lidar and resonance Doppler wind lidar (commonly used for mesospheric sodium layer measurements). For further reading, refer to References [1] and [2].

This document describes the use of heterodyne pulsed Doppler lidar systems. Some general information on continuous-wave Doppler lidar can be found in Annex A. An International Standard on this method is in preparation.

Air quality — Environmental meteorology —

Part 2: Ground-based remote sensing of wind by heterodyne pulsed Doppler lidar

1 Scope

This document specifies the requirements and performance test procedures for heterodyne pulsed Doppler lidar techniques and presents their advantages and limitations. The term "Doppler lidar" used in this document applies solely to heterodyne pulsed lidar systems retrieving wind measurements from the scattering of laser light onto aerosols in the atmosphere. A description of performances and limits are described based on standard atmospheric conditions.

This document describes the determination of the line-of-sight wind velocity (radial wind velocity).

NOTE Derivation of wind vector from individual line-of-sight measurements is not described in this document since it is highly specific to a particular wind lidar configuration. One example of the retrieval of the wind vector can be found in Annex B.

This document does not address the retrieval of the wind vector.

This document may be used for the following application areas:

— meteorological briefing for, e.g. aviation, airport safety, marine applications and oil platforms;

— wind power production, e.g. site assessment and power curve determination;

— routine measurements of wind profiles at meteorological stations;

— air pollution dispersion monitoring;

— industrial risk management (direct data monitoring or by assimilation into micro-scale flow models);

— exchange processes (greenhouse gas emissions).

This document addresses manufacturers of heterodyne pulsed Doppler wind lidars, as well as bodies testing and certifying their conformity. Also, this document provides recommendations for the users to make adequate use of these instruments.

2 Normative references

There are no normative references in this document.

3 Terms and definitions

For the purposes of this document, the following terms and definitions apply.

ISO and IEC maintain terminological databases for use in standardization at the following addresses:

— IEC Electropedia: available at http://www.electropedia.org/

— ISO Online browsing platform: available at http://www.iso.org/obp

3.1
data availability
ratio between the actual considered measurement data with a predefined data quality and the number of expected measurement data for a given *measurement period* (3.10)

3.2
displayed range resolution
constant spatial interval between the centres of two successive *range gates* (3.13)

Note 1 to entry: The displayed range resolution is also the size of a range gate on the display. It is determined by the range gate length and the overlap between successive gates.

3.3
effective range resolution
application-related variable describing an integrated range interval for which the target variable is delivered with a defined uncertainty

[SOURCE: ISO 28902-1:2012, 3.14]

3.4
effective temporal resolution
application-related variable describing an integrated time interval for which the target variable is delivered with a defined uncertainty

[SOURCE: ISO 28902-1:2012, 3.12, modified.]

3.5
extinction coefficient
α
measure of the atmospheric opacity, expressed by the natural logarithm of the ratio of incident light intensity to transmitted light intensity, per unit light path length

[SOURCE: ISO 28902-1:2012, 3.10]

3.6
integration time
time spent in order to derive the line-of-sight velocity

3.7
maximum acquisition range
R_{MaxA}
maximum distance to which the lidar signal is recorded and processed

Note 1 to entry: It depends on the number of acquisition points and the sampling frequency.

3.8
minimum acquisition range
R_{MinA}
minimum distance from which the lidar signal is recorded and processed

Note 1 to entry: If the minimum acquisition range is not given, it is assumed to be zero. It can be different from zero, when the reception is blind during the pulse emission.

3.9
maximum operational range
R_{MaxO}
maximum distance to which a confident wind speed can be derived from the lidar signal

Note 1 to entry: The maximum operational range is less than or equal to the maximum acquisition range.

Note 2 to entry: The maximum operational range is defined along an axis corresponding to the application. It is measured vertically for vertical wind profiler. It is measured horizontally for scanning lidars able to measure in the full hemisphere.

Note 3 to entry: The maximum operational range can be increased by increasing the measurement period and/or by downgrading the range resolution.

Note 4 to entry: The maximum operational range depends on lidar parameters but also on atmospheric conditions.

3.10
measurement period
interval of time between the first and last measurements

3.11
minimum operational range
R_{MinO}
minimum distance where a confident wind speed can be derived from the lidar signal

Note 1 to entry: The minimum operational range is also called blind range.

Note 2 to entry: In pulsed lidars, the minimum operational range is limited by the stray light in the lidar during pulse emission, by the depth of focus, or by the detector transmitter/receiver switch time. It can depend on pulse duration (T_{p}) and range gate width (RGW).

3.12
physical range resolution
width (full width at half maximum) of the *range weighting function* (3.15)

3.13
range gate
width (FWHM) of the weighting function selecting the points in the time series for spectral processing and wind speed computation

Note 1 to entry: The range gate is centred on the measurement distance.

Note 2 to entry: The range gate is defined in number of bins or equivalent distance range gate.

3.14
range resolution
equipment-related variable describing the shortest range interval from which independent signal information can be obtained

[SOURCE: ISO 28902-1:2012, 3.13]

3.15
range weighting function
weighting function of the radial wind speed along the line of sight

3.16
temporal resolution
equipment-related variable describing the shortest time interval from which independent signal information can be obtained

[SOURCE: ISO 28902-1:2012, 3.11]

3.17
velocity bias
maximum instrumental offset on the velocity measurement

Note 1 to entry: The velocity bias has to be minimized with adequate calibration, for example, on a fixed target.

3.18
velocity range
range determined by the minimum measurable wind speed, the maximum measurable wind speed and the ability to measure the velocity sign, without ambiguity

Note 1 to entry: Depending on the lidar application, velocity range can be defined on the radial wind velocity (scanning lidars) or on horizontal wind velocities (wind profilers).

3.19
velocity resolution
instrumental velocity standard deviation

Note 1 to entry: The velocity resolution depends on the pulse duration, the carrier-to-noise ratio and integration time.

3.20
wind shear
variation of wind speed across a plane perpendicular to the wind direction

4 Fundamentals of heterodyne pulsed Doppler lidar

4.1 Overview

A pulsed Doppler lidar emits a laser pulse in a narrow laser beam (see Figure 1). As it propagates in the atmosphere, the laser radiation is scattered in all directions by aerosols and molecules. Part of the scattered radiation propagates back to the lidar; it is captured by a telescope, detected and analysed. Since the aerosols and molecules move with the atmosphere, a Doppler shift results in the frequency of the scattered laser light.

At the wavelengths (and thus frequencies) relevant to heterodyne (coherent) Doppler lidar, it is the aerosol signal that provides the principle target for measurement of the backscattered signal.

The analysis aims at measuring the difference, Δf, between the frequencies of the emitted laser pulse, f_t, and of the backscattered light, f_r. According to the Doppler's equation, this difference is proportional to the line-of-sight wind component, as shown in Formula (1):

$$\Delta f = f_r - f_t = -2v_r/\lambda \quad (1)$$

where

λ is the laser wavelength;

v_r is the line-of-sight wind component (component of the wind vector, $\vec{v}$, along the axis of laser beam, counted positive when the wind is blowing away from the lidar).

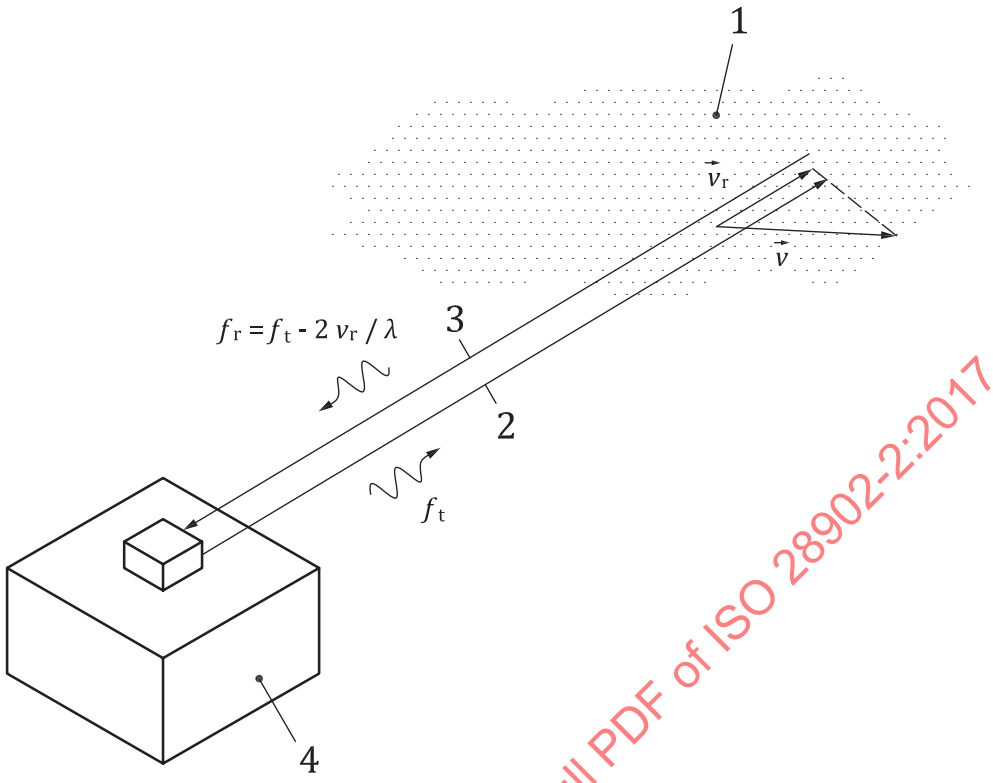

Key

1 scattering particles moving with the wind
2 optical path of the emitted laser pulse (laser beam)
3 optical axis of the receiver
4 lidar instrument

Figure 1 — Measurement principle of a heterodyne Doppler lidar

The measurement is range resolved as the backscattered radiation, received at time t after the emission of the laser pulse, has travelled from the lidar to the aerosols at range x and back to the lidar at the speed of light, c. Formula (2) shows the linear relationship between range and time.

$$x = c \cdot \frac{t}{2} \tag{2}$$

4.2 Heterodyne detection

In a heterodyne lidar, the detection of the light captured by the receiving telescope (at frequency $f_r = f_t + \Delta f$) is described schematically in Figure 2. The received light is mixed with the beam of a highly stable, continuous-wave laser called the local oscillator. The sum of the two electromagnetic waves — backscattered and local oscillator — is converted into an electrical signal by a quadratic detector (producing an electrical current proportional to the power of the electromagnetic wave illuminating its sensitive surface). An analogue high-pass filter is then applied for eliminating the low-frequency components of the signal.

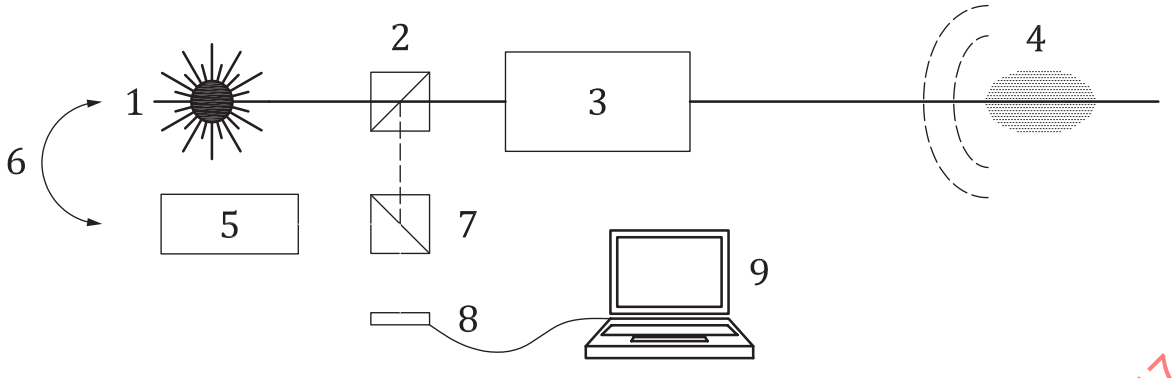

Key

1 pulsed laser
2 optical element separating the received and emitted lights
3 telescope (used for transmitting and receiving)
4 scatterers
5 local oscillator laser (continuous wave laser)
6 frequency control loo (this device sets the difference, $f_t - f_{lo}$)
7 optical element aligning the beam of the local oscillator along the optical axis of the received light beam and mixing them together
8 quadratic detector
9 analogue to digital converter and digital signal processing unit

Figure 2 — Principle of the heterodyne detection

The result is a current, $i(t)$, beating at the radio frequency, $f_t + \Delta f - f_{lo}$:

$$\underbrace{i(t) = 2 \cdot \frac{\eta \cdot e}{h \cdot f_t} \cdot K \cdot \xi(t) \cdot \sqrt{\gamma(t) \cdot P_r(t) \cdot P_{lo}} \cdot \cos\left[2\pi\left(\Delta f + f_t - f_{lo}\right) \cdot t + \varphi(t)\right] + n(t)}_{i_{het}(t)} \quad (3)$$

where

t is the time;

h is the Planck constant;

η is the detector quantum efficiency;

e is the electrical charge of an electron;

K is the instrumental constant taking into account transmission losses through the receiver;

$\xi(t)$ is the random modulation of the signal amplitude by speckles effect (see 4.5.2);

$\gamma(t)$ is the heterodyne efficiency;

$P_r(t)$ is the power of the backscattered light;

P_{lo} is the power of the local oscillator;

f_{lo} is the frequency of the local oscillator;

$\varphi(t)$ is the random phase;

$n(t)$ is the white detection noise;

$i_{het}(t)$ is the heterodyne signal.

The heterodyne efficiency, $\gamma(t)$, is a measure for the quality of the optical mixing of the backscattered and the local oscillator wave fields on the surface of the detector. It cannot exceed 1. A good heterodyne efficiency requires a careful sizing and alignment of the local oscillator relative to the backscattered wave. Optimal mixing conditions are discussed in Reference [3]. The heterodyne efficiency is not a purely instrumental function, it also depends on the refractive index turbulence (Cn^2) along the laser beam (see Reference [4]). Under conditions of strong atmospheric turbulence, the effect on varying the refractive index degrades the heterodyne efficiency. This can happen when the lidar is operated close to the ground during a hot sunny day.

In Formula (4), $P_r(t)$ is the instantaneous power of the backscattered light. It is given by the lidar equation (see Reference [3]).

$$P_r(t) = A \cdot \int_0^{+\infty} x^{-2} \cdot G(x) \cdot g\left(t - \frac{2x}{c}\right) \cdot \beta(x) \cdot \tau^2(x)\,dx \tag{4}$$

with

$$\tau(x) = \exp\left[-\int_0^x \alpha(\zeta)\,d\zeta\right]$$

where

x is the distance to the lidar;

A is the collecting surface of the receiving telescope;

$G(x)$ is the range-dependent sensitivity function ($0 \le G(x) \le 1$) taking into account, e.g. the attenuation of the receiver efficiency at short range to avoid the saturation of the detector;

$g(t)$ is the envelope of the laser pulse power ($\int g(t)\,dt = E_0$, with E_0 as the energy of the laser pulse);

$\beta(x)$ is the backscatter coefficient of the probed atmospheric target;

$\tau(x)$ is the atmospheric transmission as a function of the extinction coefficient, α.

4.3 Spectral analysis

The retrieval of the radial velocity measurement from heterodyne signals requires a frequency analysis. This is done in the digital domain after analog-to-digital conversion of the heterodyne signals. An overview of the processing is given in Figure 3. The frequency analysis is applied to a time window $(t, t + \Delta t)$ and is repeated for a number, N, of lidar pulses. The window defines a range gate $(x, x + \Delta x)$ with $x = c \cdot t/2$ and $\Delta x = c \cdot \Delta t/2$. N is linked to the integration time, $t_{int} = 1/f_{PRF}$, of the measurement (f_{PRF} is the pulse repetition frequency). The signal analysis consists in averaging the power density functions of the range gated signals. A frequency estimator is then used for estimating the central frequency of the signal peak. It is an estimate, $\hat{f}_{het}$, or the frequency, $f_{het} = \Delta f + f_t - f_{lo}$, of the heterodyne signal (see Figure 3).

Due to the analog-to-digital conversion, the frequency interval resolved by the frequency analysis is limited to $(0, +F_s/2)$ or $(-F_s/2, +F_s/2)$ for complex valued signals. This limits the minimum and maximum

values of $\hat{f}_{het}$ and thus the interval of measurable radial velocities. As shown in Reference [5], Formula (5) estimates a range-gate average of the true wind radial velocity:

$$\hat{v}_r = -\frac{\lambda}{2}\left(\hat{f}_{het} - f_t + f_{lo}\right) \tag{5}$$

For instance, in the case the signal is real valued (no complex-demodulation), the frequency offset $f_t - f_{lo}$ is set to about $F_s/4$, so $\left|\hat{v}_r\right| \le \lambda F_s / 8$. Alternatively, a system specification requiring the possibility to measure radial winds up to v_{max} commands $F_s \ge 8v_{max}/\lambda$.

The averaging kernel is the convolution function between the pulse profile and the range-gate profile. Its length is a function of the pulse footprint in the atmosphere, Δr [see Formula (6)], of the range gate, Δx, and of the weighting factor, κ, where κ is the ratio between the gate full width at half maximum (FWHM) and Δx.

$$\Delta r = \frac{c \cdot T_p}{2} \tag{6}$$

where

T_p is the FWHM duration of the laser pulse instantaneous intensity, $g(t)$.

The range resolution, ΔR, is defined as the FWHM of the averaging kernel. For a Gaussian pulse and an unweighted range gate, ΔR is calculated according to Formula (7)[6]:

$$\Delta R = \frac{c}{2} \cdot \frac{\Delta t}{\operatorname{erf}\left(\frac{\sqrt{\pi} \cdot \Delta t}{2T_p}\right)} = \frac{\Delta x}{\operatorname{erf}\left(\frac{\sqrt{\pi} \cdot \Delta x}{2\Delta r}\right)} \tag{7}$$

For a Gaussian pulse and a Gaussian weighted range gate, ΔR is equal to Formula (8):

$$\Delta R = \frac{c}{2} \cdot \sqrt{T_p^2 + \left(\kappa \cdot \Delta t\right)^2} = \sqrt{\Delta r^2 + \left(\kappa \cdot \Delta x\right)^2} \tag{8}$$

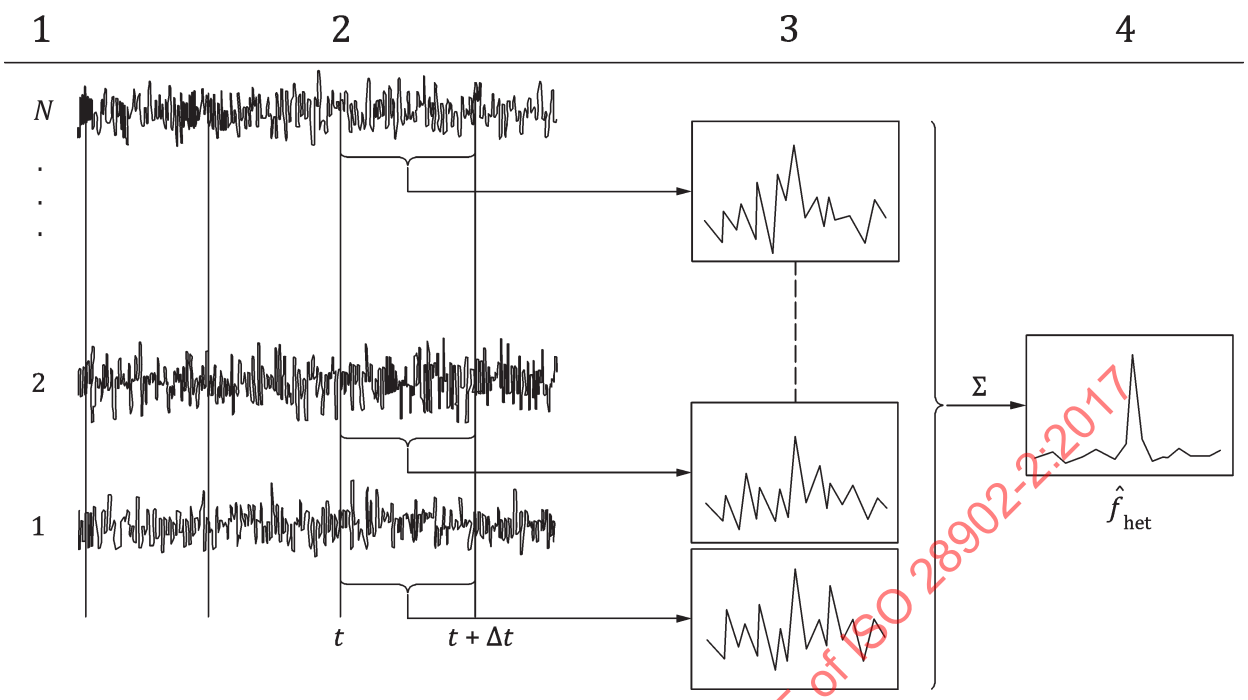

Key

t	time elapsed since the emission of the laser pulse
Δt	duration of the spectral analysis time window (it sets the size of the range gate)
N	signal number
1	pulses
2	time series
3	spectra
4	Doppler frequency

Figure 3 — Diagram showing how the frequency analysis is conducted

Several signals are considered and range gated. The average spectrum is computed and a frequency estimator is applied.

Successive range gates can be partially overlapping (then successive radial velocity measurements are partially correlated), adjacent or disjoint (then there is a "hole" in the line-of-sight profile of the radial velocity).

Several possible frequency estimators are presented in Reference [6] with a first analysis of their performances. Their performances are further discussed in Reference [7]. Whatever the estimator, the probability density function of the estimates is the sum of a uniform distribution of "bad" estimates (gross errors) spread across the entire band $[-f_{max}, f_{max}]$ and a relatively narrow distribution of good estimates often modelled by a Gaussian distribution, as shown in Formula (9):

$$p\left(\hat{f}_{het}\right) = \begin{cases} \dfrac{b}{2f_{max}} + \dfrac{1-b}{\sqrt{2\pi}\sigma_f} \exp\left(-\dfrac{\left(\hat{f}_{het} - \bar{f}_{het}\right)^2}{2\sigma_f^2}\right) & \text{for } \hat{f}_r \in \left[-f_{max}, f_{max}\right] \\ 0 \quad \text{otherwise} \end{cases} \tag{9}$$

In principle, the mean frequency, $\bar{f}_{het}$, can be different from the "true" heterodyne signal frequency, f_{het}. This can happen for instance when the frequency drifts during the laser pulse (chirp, see Reference [8]). However, these conditions are rarely met and a good heterodyne Doppler lidar produces in practice un-biased measurements of Doppler shifts.

The parameter σ_f characterizes the frequency precision of the estimator. The corresponding radial velocity precision is $\sigma_v = \lambda \cdot \sigma_f/2$. In a heterodyne system, it is typically of the order of several to several tens of centimetres per second. It degrades with the level of noise [power of $n(t)$ in Formula (3)] and improves with the number of accumulated signals, N. In practice the improvement is limited as the accumulation of a large number of signals result in a long integration time during which the natural variability (turbulence) of the wind increases.

Reference [9] discusses the presence of gross errors (also called outliers[1]) and proposes a model for the parameter b as a function of the several instrument characteristics and the level of detection noise. An outlier happens when the signal processor detects a noise peak instead of a signal peak. The parameter b is a decreasing function of the CNR. Quality checks shall be implemented in heterodyne lidar systems so gross errors are filtered out and ignored as missing data. The presence of gross errors sets the maximum range of the lidar.

4.4 Target variables

The aim of heterodyne Doppler wind lidar measurements is to characterize the wind field. In each range interval, the evaluation of the measured variable leads to the radial velocity; see Formula (5).

There are additional target values like the variability of the radial velocity that are not discussed in this document.

The target variables can be used as input to different retrieval methods to derive meteorological products like the wind vector at a point or on a line (profile), in an arbitrary plane or in space as a whole. This also includes the measurement of wind shears, aircraft wake vortices (see Figure C.1), updraft and downdraft regions of the wind. An additional aim of the Doppler wind lidar measurements is to determine kinematic properties and parameters of inhomogeneous wind fields such as divergence and rotation. See examples of applications in Annex C.

4.5 Sources of noise and uncertainties

4.5.1 Local oscillator shot noise

The shot noise is denoted $n(t)$ in Formula (3). Its variance is proportional to the local oscillator (LO) power, as shown in Formula (10):

$$\left\langle n^2{}_{SN} \right\rangle = 2eSP_{lo}B \tag{10}$$

where

S is the detector sensitivity, $S = \dfrac{\eta e}{hf_t}$, where η is the detector quantum efficiency;

B is the detection bandwidth.

It causes gross errors and limits the maximum range of the signal. If no other noise source prevails, the strength of the heterodyne signal relative to the level of noise is measured by the carrier-to-noise ratio, CNR, as shown in Formula (11)[6]:

$$\mathrm{CNR} = \frac{\eta \cdot K \cdot \gamma(t)}{h \cdot f_t \cdot B} P_r(t) \tag{11}$$

NOTE Some authors sometimes call signal-to-noise ratio (SNR) what is defined here as the carrier-to-noise ratio (CNR).

4.5.2 Detector noise

Additional technical sources of noise can affect the SNR. As the shot noise, their spectral density is constant along the detection bandwidth (white noise).

— Dark noise is created by the fluctuations of the detector dark current, i_D, as shown in Formula (12):

$$\left\langle n^2{}_{DN} \right\rangle = 2e\, i_D B \tag{12}$$

— Thermal noise (Johnson/Nyquist noise) is the electronic noise generated by the thermal agitation of the electrons inside the load resistor, R_L, at temperature T, as shown in Formula (13):

$$\left\langle n^2{}_{TN} \right\rangle = \frac{4k_B T}{R_L} B \tag{13}$$

where

k_B is the Boltzman constant.

4.5.3 Relative intensity noise (RIN)

The RIN (dB/Hz) is the LO power noise normalized to the average power level. RIN typically peaks at the relaxation oscillation frequency of the laser then falls off at higher frequencies until it converges to the shot noise level. (pink noise). The RIN noise current increases with the square of LO power.

$$n^2{}_{\mathrm{RIN}} = \left(SP_{\mathrm{lo}}\right)^2 10^{0,1\,\mathrm{RIN}}\, B \tag{14}$$

In a good lidar system, i_D RIN, $1/R_L$ are low enough so that the LO shot noise is the prevailing source of noise. In that case only, Formula (14) is applicable.

4.5.4 Speckles

The heterodyne signal for a coherent Doppler wind lidar is the sum of many waves backscattered by individual aerosol particles. As the particles are randomly distributed along the beam in volumes much longer than the laser wavelength, the backscattered waves have a random phase when they reach the sensitive surface of the detector. They, thus, add randomly. As a result, the heterodyne signal has a random phase and amplitude. The phenomenon is called speckles (see Reference [10]). It limits the precision of the frequency estimates.

4.5.5 Laser frequency

A precise measurement of the radial velocity requires an accurate knowledge of $f_r - f_{lo}$. Any uncertainty in this value results in a bias in $\hat{f}_r$. If the laser frequency, f_t, is not stable, it should either be measured or locked to f_{lo}.

4.6 Range assignment

The range assignment of Doppler measurements is based on the time elapsed since the emission of the laser pulse. This time shall be measured with a good accuracy (the error, ε_t, shall be smaller or equal than $2\delta \cdot x/c$, where $\delta \cdot x$ is the required precision on the range assignment). This requires, in particular, that the time of the laser pulse emission is determined with at least this precision.

4.7 Known limitations

Doppler lidars rely on aerosol backscatter. Aerosols are mostly generated at ground and lifted up to higher altitudes by convection or turbulence. They are, therefore, in great quantities in the planetary

boundary layer (typically 1 000 m thick during the day in tempered areas, 3 000 m in tropical regions), but in much lower concentrations above. It follows Doppler lidars hardly measure winds above the planetary boundary layer except in the presence of higher altitude aerosol layers like desert dusts or volcanic plumes.

Laser beams are strongly attenuated in fogs or in clouds. It follows the maximum range of Doppler lidars is strongly limited in fogs (a few hundreds of metres at best) and cannot measure winds inside or beyond a cloud. They are able to penetrate into subvisible clouds as cirrus clouds. Therefore, wind information at high altitude (8 km to 12 km) can be retrieved from crystal particle backscattering.

Doppler lidars detect cloud water droplets or ice crystals when they are present in the atmosphere. As they are efficient scatterers, they may dominate the return from the atmosphere, in case of heavy precipitation, for example, in which case the Doppler lidar measures the radial velocity of hydrometeors rather than the radial wind.

Rain downwashes the atmosphere, bringing aerosols to the ground. The range of a Doppler lidar is generally significantly reduced after a rain, before the aerosols are lifted again.

The presence of rain water on the window of a Doppler lidar strongly attenuates its transmission. Unless a lidar is equipped with a wiper or a blower, its window should be wiped manually.

As explained in 4.2, the efficiency of heterodyne detection is degraded by the presence of refractive index turbulence along the beam. Refractive index turbulence is mostly present near the surface during sunny days. The maximum range of Doppler lidar looking horizontally close to the surface may thus be substantially degraded in such conditions.

5 System specifications and tests

5.1 System specifications

5.1.1 Transmitter characteristics

5.1.1.1 Laser wavelength

The laser wavelength depends mainly on the technology used to build the laser source. Most of the existing techniques use near-infrared wavelengths between 1,5 µm to 2,1 µm, even though other wavelengths up to 10,6 µm may be used. The choice of the wavelength takes into account the expected power parameters but also the atmospheric transmission and the laser safety (see References [11] and [12]). In fact, the choice of the window between 1,5 µm and 2,1 µm is a compromise between technology and safety considerations (>1,4 µm to ensure eye safety).

5.1.1.2 Pulse duration

The laser pulse duration, T_p, is the FWHM of the laser pulse envelope, $g(t)$. T_p defines the atmosphere probed length, R_p, contributing to the instantaneous lidar signal, as shown in Formula (15):

$$R_p = \frac{c \cdot T_p}{2} \tag{15}$$

As an example, a pulse duration of 200 ns corresponds to a probed length of approximately 30 m.

5.1.1.3 Velocity precision and range resolution vs. pulse duration

There is a critical relationship between the pulse duration and two performance-related features. A long pulse duration of several hundreds of nanoseconds leads to a potentially narrow FWHM of the laser pulse spectrum (if "chirping" can be avoided), (see the Fourier transform of the overall pulse in the time domain). This can lead to a very accurate wind measurement even for a very low signal-to-noise ratio

provided that outliers can be avoided (see 4.3). There is an adverse impact from high performance on range resolution. A pulse duration of 1 µs limits the effective range resolution to approximately 150 m [see Formula (6)].

5.1.1.4 Pulse repetition frequency

The pulse repetition frequency, f_{PRF}, is the laser pulse emission frequency. f_{PRF} determines the number of pulses sent and averaged per line of sight in the measurement time. It also determines the maximum unambiguous range where the information of two consecutive sent laser pulses will not overlap. The maximum unambiguous range, R_{MaxO}, corresponds to f_{PRF} as in Formula (16):

$$R_{MaxO} = \frac{c}{2 f_{PRF_{max}}} \tag{16}$$

For example, for a maximum operational range of 15 km, the maximum f_{PRF} is 10 kHz.

As for radars, however, specific types of modulation (carrier frequency, repetition frequency, etc.) can overcome the range ambiguity beyond R_{MaxO}.

5.1.2 Transmitter/receiver characteristics

The transmitter/receiver is defined at least by the parameters given in Table 1.

Table 1 — Transmitter/receiver characteristics

Transmitter/receiver characteristics	Remarks
Aperture diameter	Physical size of the instrument's aperture that limits transmitted and received beams
Laser beam diameter and truncation factor	For a Gaussian beam, the laser beam diameter is defined as the diameter measured at $1/e^2$ in power at the lidar aperture. The laser beam diameter defines the illuminance level and so the eye safety. The truncation factor is the ratio between the diameter measured at $1/e^2$ and the physical size of the instrument's aperture.
Focus point	Usually, pulsed lidars use collimated beams. For some applications, the beam can be partially focused at a given point to maximize the intensity on the beam laser within the measurement range. The intensity of the signal, and thus the velocity accuracy, will be optimized at this specific point.

In principle, pulsed systems are monostatic systems. For continuous wave systems, bistatic setups are also available.

5.1.3 Signal sampling parameters

The sampling of the pulsed lidar signal in range is determined by the parameters given in Table 2.

Table 2 — Signal sampling parameters

Signal sampling parameters	Remarks
Range gating	The range gate positions can be defined along the line of sight.
Range gate width	Given by the sampling points or the sampling frequency of the digitizer. Should be chosen close to the pulse length.
Number of range gates	For real-time processing, spectral estimation of all range gates shall be computed in a time less than the integration time.
Radial window velocity measurement range	Wind velocities as low as 0,1 m/s can be measured with the aid of Doppler wind lidar systems. The measurement range is restricted towards the upper limit only by the technical design, mainly by the detection bandwidth. A radial wind velocity range of more than 70 m/s can be measured.
Resolution of the radial velocity	The wind velocity resolution is the minimum detectable difference of the wind velocity in a time and range interval. A resolution of 0,1 m/s or better can be achieved by averaging.

5.1.4 Pointing system characteristics

The pointing system characteristics are given in Table 3.

Table 3 — Pointing system characteristics

Pointing system characteristics	Remarks
Azimuth range	When using a pointing device, a lidar has the capability to point its laser beam at various azimuth angles with a maximum angular capability of 2π. For endless steering equipment, a permanent steering along the vertical axis is allowed. Other scanning scenarios should be followed for non-endless rotation gear.
Elevation range	The pointing device can be equipped with a rotation capability around the horizontal axis. Potential 360° rotation can be addressed. Typical elevation angles are set from 0° to 180° in order to observe the semi-hemispherical part of the atmosphere above the lidar. Anyhow, a nadir pointing can be used for resting position of the equipment.
Angular velocity	The angular velocity is the speed at which a pointing device is rotating. A measurement can be performed during this rotation. In this case, the wind velocity information will be a mean of the various lines of sights in the probed area, between a starting angle and a stopping angle. Other scenarios of measurement can use a so-called step and stare strategy, with a fixed position during the measurement.

Table 3 *(continued)*

Pointing system characteristics	Remarks
Angular acceleration	Defines how fast the angular velocity can change. To be defined for complex trajectories with fast changes in direction. Angle overshoots can be observed at high angular acceleration.
Pointing accuracy	The relative pointing accuracy is the standard deviation of the angular difference between the actual line-of-sight position (azimuth and elevation) and the position of the target (system of reference of the instrument). The absolute pointing accuracy needs prior calibration by angular sensors (pitch, roll, heading) (system of geographical reference).
Angular resolution	Minimum angle step that the line of sight can move. It can be limited by a motor reduction factor, position, encoder or mechanical friction.

5.2 Relationship between system characteristics and performance

5.2.1 Figure of merit

A figure of merit (FOM) helps to compare range performance of different lidars with different parameters. The example shown in Figure 4 allows the classification of pulsed lidar sensitivities, independently of atmospheric parameters. FOM is derived from the lidar equation [see Formula (4)] and is proportional to velocity spectrum, CNR, which is defined on the averaged spectral density as the Doppler peak intensity divided by the spectral noise standard deviation, assumed to be constant (white noise). N is the number of averaged pulses.

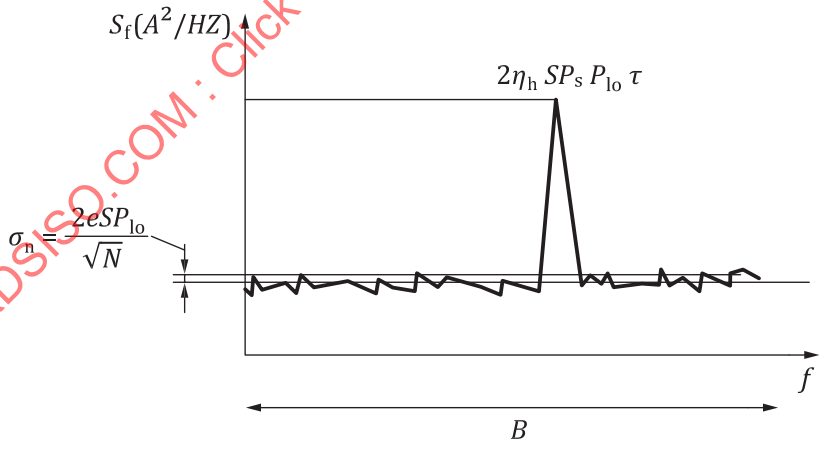

Figure 4 — Example of FOM

FOM is defined for a set of lidar parameters as in Formula (17):

$$\mathrm{FOM} = \eta_{\mathrm{all}} \cdot E \cdot T_{\mathrm{p}} \cdot D^2 \cdot \sqrt{t_i \cdot f_{\mathrm{PRF}}} \tag{17}$$

where

η_{all} is the overall efficiency, taking into account beam and image quality, overall transmission and truncation factor;

E is the laser energy at the laser output (received energy is proportional to peak power and laser footprint);

T_p is the pulse duration (this term comes from narrow bandwidth, inversely proportional to T_p);

D is the collecting telescope diameter (for typical long range applications, the optimum is 100 mm to 150 mm in size for NIR wavelengths);

t_i is the integration time for one line of sight;

f_{PRF} is the pulse repetition frequency.

The FOM is proportional to the square root of number N of accumulated spectra: $N = t_i f_{PRF}$.

When comparing two lidars at two different wavelengths, spectral dependence of atmospheric parameters should be considered. The FOM shall be calculated with an integration time less or equal to 1 s to avoid that wind or turbulence may fluctuate more than the Doppler spectral width.

A lidar may increase its FOM with a longer accumulation time within this 1 s time limit.

Considering state-of-the-art low aberration optical components, η_{all} can be estimated by the product of the emitting path transmission by the receiving path transmission.

It has to be noted that the FOM for a pulsed Doppler lidar may not be increased indefinitely by increasing the collecting area, D^2, since phase distortion across the beam due to refractive index turbulence degrades the heterodyne efficiency[3]. A practical limit is in the vicinity of D = 125 mm useable diameter for long range lidars.

Since the velocity spectrum CNR is inversely proportional to the squared range, the maximum operational range is approximately proportional to the square root of FOM, when atmospheric absorption can be neglected. When FOM is expressed in mJ ns m^2, the maximum operational range, expressed in km, is almost the square root of FOM.

Table 4 computes the FOM for typical lidar figures and their corresponding typical measurement range.

Table 4 — Figure of merit for typical lidar figures and their corresponding typical measurement range

η	E	T_p	D	f_{PRF}	t_i	FOM	**Typical measurement range**
	mJ	ns	m	Hz	s	mJ ns m^2	km
0,5	0,2	800	0,12	10 000	1	115	10
0,5	0,1	400	0,06	20 000	1	10	3
0,5	2	300	0,12	750	1	118	10

5.2.2 Time-bandwidth trade-offs

A good practice is to match the pulse duration with the desired range gate (see 4.6) so that the spatial resolution depends equally on these two parameters. With this assumption, spatial resolution is proportional to pulse duration. The shorter the pulse, the better the resolution. Velocity resolution is proportional to spectrum width and is larger when the spectrum is narrow. Because the spectrum width is inversely proportional to the pulse duration, range resolution and velocity resolution are also inversely proportional.

5.3 Precision and availability of measurements

5.3.1 Radial velocity measurement accuracy

Radial velocity measurement accuracy is defined (according to ISO 5725-1) in terms of

— trueness (or bias) as the statistical mean difference between a large number of measurements and the true value, and

— precision (or uncertainty) as the statistical standard deviation of a series of independent measurements. It does not relate to the true value.

Lidar data of good quality are obtained when the precision of the radial velocity measurements is higher than a target value (e.g. 1 m/s) with a predefined probability of occurrence (e.g. 95 %).

An error value (1σ) of 0,5 m/s can be regarded as adequate for typical meteorological applications and for wind measurements to determine the statistics of dispersion categories for air pollution modelling[13]. For wind energy applications, the requirements may be higher (0,2 m/s).

5.3.2 Data availability

Data availability is defined as the ratio of data with precision, *P*, to the total number of data during a measurement period.

The availability of measurement data, i.e. the determinability of the wind profile is a function mainly of the aerosol concentration and the clouds. Other filtering criteria may be applied, depending on the required data accuracy. For example, data that exhibits significantly non-uniform flow around the scan disk should be rejected.

5.3.3 Maximum operational range

Assuming the lidar line of sight remains within the planetary boundary layer (i.e. no significant change of signal along the line of sight), Figure 5 shows a typical pulsed lidar data availability versus range plot.

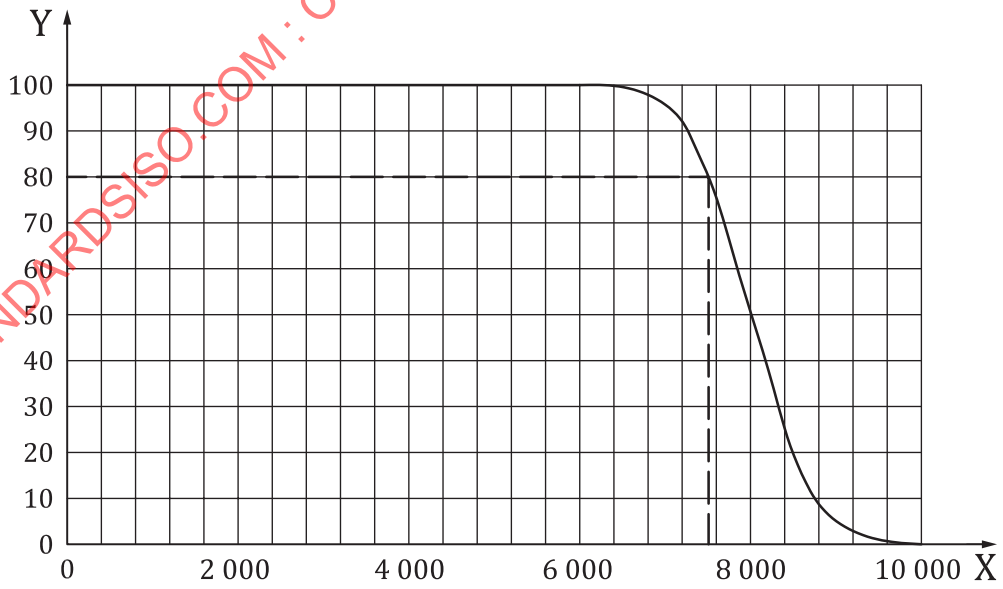

Key

X range in metres

Y availability in %

Figure 5 — Example for maximum operational range

In this case, the range for 80 % data availability (P_{80}) is 7 500 m.

The performance shown in this diagram is based on a standard atmosphere:

— no clouds along the line of sight;

— no precipitation;

— visibility over 10 km (clear air).

This performance will vary significantly with relevant local climatic and operational conditions. Data from greater ranges should be treated with caution, depending on the application.

Measurement range shall be defined with a given availability criteria. Recent study about this link is described in Reference [14].

For example, R_{50} corresponds to the maximum range with availability over 50 %.

If the availability is not mentioned, the maximum operational range is supposed to be R_{80}, i.e. the maximum distance where the availability is over 80 %.

For a given availability, a change in velocity precision leads to a change in maximum operational range.

5.4 Testing procedures

5.4.1 General

In order to accurately assess for the accuracy of the target variables, the manufacturer should perform a set of validation tests for the range and velocity. Some can be performed under laboratory conditions. Certain other validation tests can only be performed by a comparison with other reference instruments, such as cup or sonic anemometers.

5.4.2 Radial velocity measurement validation

5.4.2.1 General

This subclause describes how the quality of radial velocity measurements can be checked and assessed.

5.4.2.2 Hard target return

This test consists in acquiring wind measurements with the beam directed to a stationary (unmoving) hard target (any building within lidar range) and checking the radial velocity measurement returned by the lidar is 0 m/s.

This test checks the frequency difference, $f_t - f_{lo}$, between emitted laser pulses and the local oscillator is known or determined with a sufficient accuracy (see 4.5.3).

The range gate length should be close to the length of the laser pulse, and the distances of the range gates should be set so that the hard target is exactly at the centre of one range gate, otherwise, a velocity bias can occur in case of frequency drift within the pulse.

Hard target velocity measurements should be acquired during at least 10 min. The test is successful if the time sequence of hard target radial velocities is centred at about 0 m/s.

5.4.2.3 Self-assessment of radial velocity precision

In this test, the pulsed lidar beam is vertical and radial velocity measurements are acquired during at least 20 min at the rate of at least one profile of radial velocities every second. Let us denote by

v_r (x,k), k = 1,...,K the time sequence of radial velocities measured at distance x. The test consists in forming the power spectrum of the time sequence, as shown in Formula (18):

$$V\left(x,f\right)=\frac{1}{K}\left|\sum_{k=1}^{K}v_r\left(x,k\right)\exp\left(-2j\pi fk\delta t\right)\right|^2 \tag{18}$$

where

δt is the constant time lag between successive v_r (x,k)measurements.

On average, the power spectrum $V(x,f)$ should look like Figure 6. At low frequencies, the power spectrum is dominated by natural wind fluctuations and shall follow a $f^{5/3}$ law. At high frequencies, the power spectrum is dominated by the flat level of measurement errors (white noise). The level of this flat part directly gives the variance of these measurements $\sigma_e^2\left(x\right)$.

NOTE The test shall be carried out at night when the natural variability of the wind is weak, i.e. when the wind is considered to be calm. It may then happen that measurement errors are much larger than natural wind fluctuations so the $f^{5/3}$ part of the power spectrum is hidden.

Fully described in Reference [15], this technique allows for the estimation of the measurement precision of the lidar without any ancillary data.

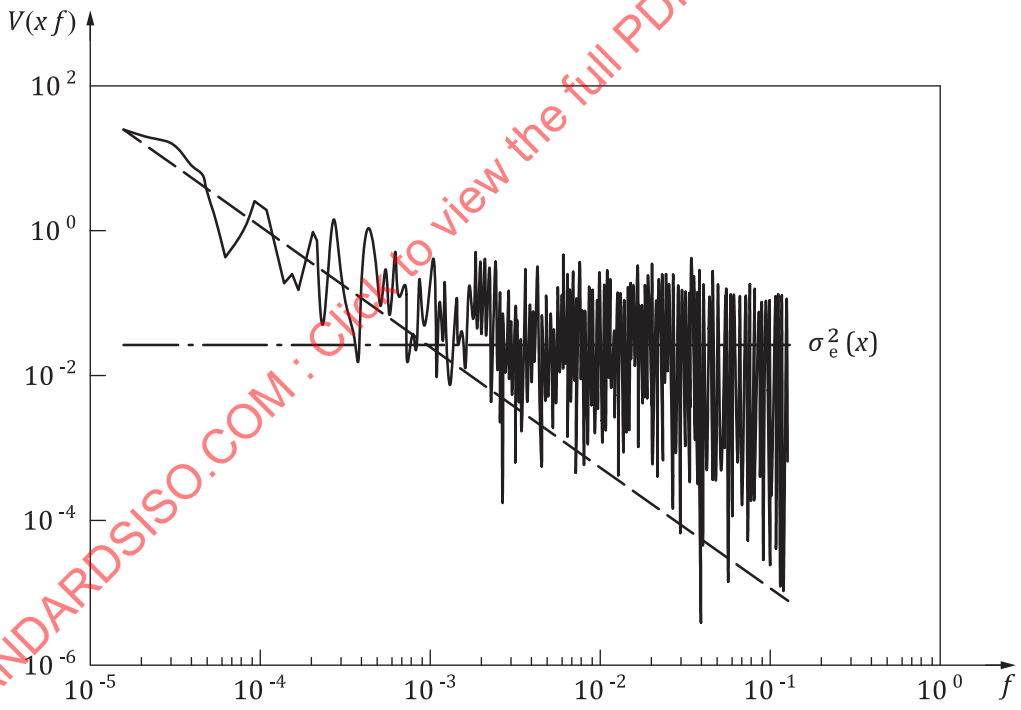

Key

f frequency

$V(x,f)$ power spectrum

Figure 6 — Power spectrum of radial velocity measurements

The line is $V(f)$. At low frequencies, $V(f)$ should be proportional to $f^{5/3}$ (spectral behaviour of natural wind variability; see dashes). At high frequencies, the spectrum becomes flat (dash-dot line) at a level directly equal to the variance of measurement errors, σ_e^2.

5.4.3 Assessment of accuracy by intercomparison with other instrumentation

5.4.3.1 Sonic anemometer

The last test consists of directing the lidar beam very close to a sonic anemometer on a mast or platform without vibration and comparing lidar radial velocities with the projection of the three-dimensional wind vectors acquired by the sonic anemometer on the beam direction.

Lidar and sonic anemometer data shall be averaged over a minute.

The direction of the lidar beam shall be determined with a good accuracy (of the order 1° or better) and as close as possible to the horizontal plane. The lidar beam shall be at the height of the sonic anemometer (height difference of the order of 1 m or less).

The root mean square of the differences between lidar and sonic anemometer data shall be less than 0,1 m/s.

The mast will most likely cause wind flow perturbations downstream. Winds coming from directions such that the sonic anemometer is in the perturbed zone shall be removed from the statistics.

5.4.3.2 Performance test against masts

The mast shall be equipped with at least three-cup anemometers mounted horizontally.

5.4.3.3 Comparison with Doppler weather radars

The possibility for inter-comparison between Doppler lidars and Doppler weather radars can be an option where the two systems are collocated. The details about this class of inter-comparison are just becoming known as the deployment of systems integrating both sensors for all-weather remote sensing of the wind field at airports, especially for wind shear detection, is just getting under way. Studies have recently been conducted[16][17][18]. Both sensors should be collocated and should probe the same atmospheric volume in order to be certain of representative inter-comparisons.

In addition to the siting requirement, it is very important that weather situations be selected in which the tracer targets of both sensors actually represent the flow of air. In conditions of dry weather, the Doppler lidar works best, while under such conditions of clear air, the radar measures only the returns due to scattering by insects. These scattered signals from insects provide no accurate indication of the actual air movement. Comparison with data from Doppler lidars typically shows differences of up to several metres per second. Therefore, echo classification in terms of radar targets has to be enabled in order to be able to reject insect returns. This means that the radar has to be capable of measuring at two orthogonal linear polarizations. During precipitation events, however, conditions are optimal for the radar, whereas, the lidar may have significantly reduced range coverage. In weather situations with light rain or drizzle from stratiform cloud, both radar and lidar sensors are expected to obtain high quality data. Such situations are thus best suited for this validation procedure. Appropriate filtering of radar data on the basis of target classification using dual polarization moments needs to be conducted in order to get rid of any non-meteorological returns.

If these requirements are fulfilled, cross comparison of Doppler weather radar and Doppler lidar can be performed on the basis of profiles of horizontal wind as obtained, e.g. with velocity volume processing (VVP) or velocity azimuth display (VAD) methods. In this case, the scan geometry has to be considered. Ideally, the scan geometry for the radar and lidar should be the same with respect to elevation angles. Another option yet to be evaluated could be to compare the actual radial wind velocities on a range gate by range gate basis between the radar and lidar systems.

5.4.3.4 Comparison with radar wind profilers

Comparison with radar wind profilers may be performed if the two systems are collocated. The weather conditions under which both sensors work optimally are not exclusive of each other (sufficient aerosol tracers for lidar and sufficient turbulent eddies as targets for Bragg scattering for the wind profiler).

Care shall be taken that both sensors face optimal atmospheric conditions. Additionally, attention has to be paid to the scan mode used to derive the vertical wind profile so that the volume probed by the lidar matches the volume probed by the wind profiler.

5.4.4 Maximum operational range validation

In clear sky conditions, the atmosphere can be described by the visibility, *V*, the aerosol concentration and the aerosol type, where the last two can be properly described by the two optical lidar parameters extinction and backscatter coefficients. The visibility (see, for example, ISO 28902-1) and humidity are measured by standard ground based meteorological local sensors, whereas, the aerosol type and its size distribution are not. To simplify, atmosphere types can be sorted in a few categories associated with their lidar ratio. Lidar ratio values in the NIR typically are limited in the range of 30 to 50 steradians. R_{MaxO} will not be too dependent on the aerosol variability on site except for conditions with local pollution sources.

Visibility is an important parameter for lidar range. The lidar equation [see Formula (4)] indicates that the received power is proportional to the backscatter coefficient and decreases exponentially with extinction, thus increases with visibility. Since $\alpha(x)$ and $\beta(x)$ are proportional, there is a maximum to the function $P_{\mathrm{r}}(t)$ (see lidar equation, Formula (4) and Figure 7), and so for R_{MaxO}.

To discard unfavourable visibility conditions for coherent Doppler wind lidars (fog and very clear), only haze and clear visibility conditions are selected for range measurements. Current lidars can work in precipitating conditions, but are subject to error in their determination of the vertical wind component; the horizontal component has been shown to be very accurate (see Reference [18]).

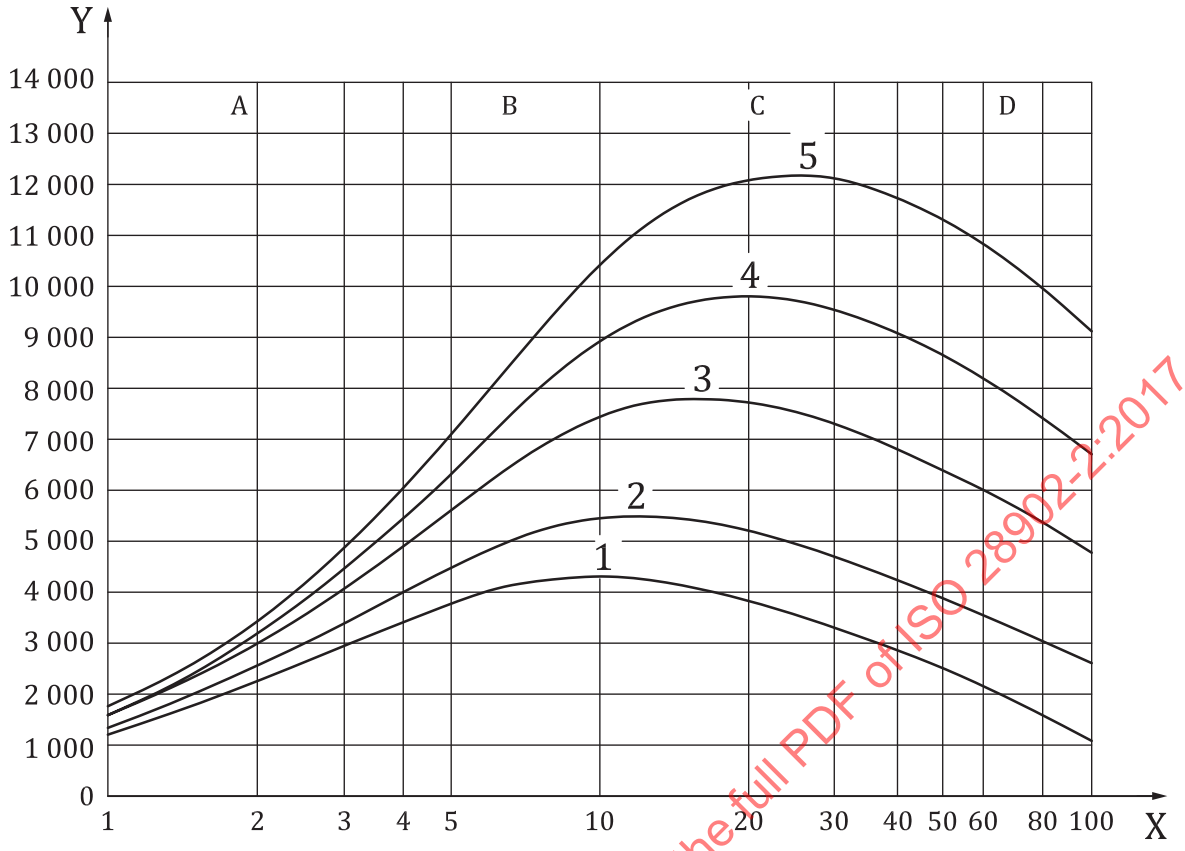

Key

X	visibility in km
Y	maximum range in metres
1 to 5	different FOM values (see Table 5)
A	fog
B	haze
C	clear
D	very clear

Figure 7 — Dependency of the maximum operational range of the heterodyne Doppler signal to the visibility conditions

Table 5 — Plot numbers

Plot number	1	2	3	4	5
Typical FOM for 1 s integration time (mJ ns m^2)	20	30	60	100	150

Because backscatter changes rapidly for high RH values, data corresponding to RH > 70 % should be filtered out the measurement data set. So, precipitation conditions (rain, snow) are not considered.

Moreover, index turbulence, Cn^2 (depends on temperature and altitude), can modify R_{MaxO} by altering the beam wave front. Strong turbulent conditions shall be removed from data sets (sunny days around noon), and experimental protocol shall be followed up.

So the validation shall be conducted under the following conditions:

— the lidar is operated in operational conditions (vertical for profilers, low elevation for scanning lidars;

— the full measurement range remains in the boundary layer;

— 10 km < visibility < 50 km (at visible wavelength, dependency with wavelength is given in ISO 28902-1);

— no precipitation;

— no cloud on the line of sight;

— $Cn^2 < 10^{-14}$ $m^{-2/3}$ (1 m above ground level).

Data not corresponding to these conditions should be filtered out for assessing the maximum operational range.

a) Context conditions are recorded simultaneously (temperature, Cn^2, visibility, RH).

b) Data sets are created following the above mentioned atmospheric conditions. 100 h of filtered data are required as a minimum for a good statistical data set. It represents around 4 days of cumulated measurements with 1 s accumulation time. Depending on the atmospheric conditions, the evaluation period can last from 4 days and up to 1 month.

6 Measurement planning and installation instructions

6.1 Site requirements

The selection of the measurement site is essentially determined by the measurement task. Careful selection of the measurement site is necessary, in particular, for stationary systems or for the quasi-stationary use of mobile systems during long-term measurement campaigns. The following points shall be taken into account when selecting the measurement site.

— Unobstructed view: Unrestricted visibility can be limited by built-up areas, trees and buildings near the installation site of the lidar. If the view is limited by buildings, it is possible to avoid the limitation of the horizontal view by selecting a larger elevation angle. In the case of a VAD scan, the measurement signals originating not from the free atmosphere but from obstacles shall be excluded from the evaluation.

— Electromagnetic radiation: Doppler wind lidar systems should be shielded properly against interferences by electromagnetic radiation (e.g. by radar, mobile radio or cellular phone networks).

Early inspection of the envisaged measurement site with the participation of experts (e.g. meteorologists) is recommended.

For optimal operational range retrieval, the lidar should be installed on a short grass-covered ground with no nearby structures, which would cause atmospheric turbulence affecting the lidar's operation and performance. The lidar should be installed at least at 3 m above the ground, especially when not located on a grass ground, like concrete, asphalt or a plain metallic platform, in order to avoid effects from turbulence nearby the optical output that will destroy the coherency of the atmosphere and thus drastically diminish the detection.

6.2 Limiting conditions for general operation

Interference factors regarding Doppler wind lidar measurements are:

— optically thick clouds;

— precipitation of any type (rain, hail, snow);

— blocking effects (e.g. buildings).

6.3 Maintenance and operational test

6.3.1 General

To ensure the system functions as specified and to rule out deviations and technical errors such as maladjustments[19], maintenance and operational tests shall be performed in regular intervals. In addition to the information given here, typical application ranges and corresponding requirements can be found in Annex D.

6.3.2 Maintenance

Maintenance such as regular cleaning of the optical components, calibration, etc. shall be performed as a basic requirement of quality assurance. Maintenance procedures may be conducted by on-site personnel, using an automatic software detection of the decrease of the signal due to, e.g. dust deposits, and making appropriate corrections to the data, or a combination of the two. Typical maintenance intervals are 3 months depending on the environmental conditions.

6.3.3 Operational test

Operational tests should be performed every 6 to 36 months. The tests depend on the individual system design. The manufacturer shall specify the testing procedures and provide the necessary testing tools.

a) Output power and frequency of the laser source should be measured at the periodicity indicated by the manufacturer.

b) Signal output of the data acquisition system reacting to a defined light pulse or defined target should be measured at the periodicity indicated by the manufacturer.

c) For scanning or steering systems, an alignment test using a calibrated instrument (e.g. compass, inclination meter) should be performed.

6.3.4 Uncertainty

Table 6 compiles uncertainty contributions to the measurement variables and the line-of-sight wind velocity. The uncertainty contributions of the measurement variables influence the quality of the data produced by the system. The dominant uncertainties result from:

— the initial calibration process of the system by the manufacturer;

— the prevailing environmental conditions.

Table 6 — Effects leading to uncertainty

Measurement variables	Effects leading to uncertainty
SNR	— Noise including detector noise — Speckle effect (when only a few pulses are averaged during the measurement time) — Laser power or pulse width fluctuations — Refractive index (temperature) turbulence — Lag angle at fast rotation speeds
Frequency shift, Δf	— Bias and fluctuations of emitted pulse frequency compared to local oscillator frequency — Pulse length — SNR — Number of averaged pulses — Quality of estimator
Target variable	**Uncertainty contribution**
line-of-sight wind velocity (radial wind velocity)	— Wind turbulence — Wind gradient along the line of sight — Hard targets close to the range gate — Range ambiguities — Pointing accuracy

Annex A
(informative)

Continuous-wave Doppler wind lidar

As stated in this document, there are several methods by which lidar can be used to measure atmospheric wind. The four most commonly used methods are pulsed and continuous-wave (CW) coherent Doppler wind lidar, direct-detection Doppler wind lidar and resonance Doppler wind lidar (most commonly used for mesospheric sodium layer measurements).

This document describes the use of heterodyne (coherent) pulsed lidar systems. It should be noted that there is also ISO 28902-3 currently in preparation, which describes the use of continuous-wave coherent Doppler wind lidar for the measurement of atmospheric wind. ISO 28902-3 will specify the requirements and performance test procedures for continuous-wave Doppler lidar techniques and presents its advantages and limitations. The term “continuous wave Doppler lidar” or “continuous wave Doppler wind lidar” is used in this document to apply to continuous-wave lidar systems making measurements of wind characteristics from the scattering of laser light by aerosols in the atmosphere within the low-altitude boundary layer. A description is provided of typical measurement geometries, signal-processing options, performance requirements, and limits based on standard atmospheric conditions. The applications for continuous wave lidar are, among others:

— wind energy;

— wind resource assessment;

— power curve verification;

— loss factor in the wind farm operation;

— wind hazards monitoring for aviation weather applications;

— wind shear;

— requirements for the detection of wake vortices behind aircraft.

ISO 28902-3 will address manufacturers of continuous-wave Doppler wind lidars, as well as those bodies concerned with the testing and certifying their conformity. It will also provide recommendations for users to make adequate appropriate use of these instruments. A comprehensive bibliography of independent publications will be provided.

Annex B
(informative)

Retrieval of the wind vector

B.1 General

The wind is a three-dimensional vector quantity, with the wind field being generally a function of space and time. The measurement of the instantaneous wind at a particular position therefore always requires the determination of three vector components. A single Doppler lidar is only able to measure the component (or projection) of the wind vector along the line of sight of the laser beam. Three separated lidar systems would therefore be required to perform an exact local measurement at any fixed time. Under certain assumptions, it is possible to estimate the full wind vector from a single "monostatic" Doppler lidar. This process is called wind retrieval since the accuracy of the wind vector estimate depends on the validity of the assumptions regarding the wind field.

B.2 Coordinate system

Figure B.1 shows the wind vector $\vec{u}\left(\vec{r},t\right)$ in the Cartesian coordinate system with the unit vectors $\vec{i}, \vec{j}, \vec{k}$. The components u_x, u_y, u_z are scalar functions of position and time, $\vec{r} = \vec{r}\left(x,y,z,t\right)$, is the position or radius vector of an air parcel.

$$\vec{u} = \frac{d\vec{r}}{dt} = \begin{pmatrix} u_x \\ u_y \\ u_z \end{pmatrix} \tag{B.1}$$

or

$$\vec{u} = \left(u_x \cdot \vec{i} + u_y \cdot \vec{j} + u_z \cdot \vec{k}\right) \tag{B.2}$$

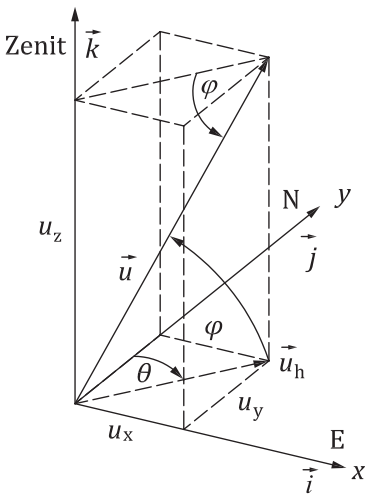

Figure B.1 — Coordinate system and wind vectors

The coordinate system in Figure B.1 points to the East (E) with the positive x-direction ($\vec{i}$), to the North (N) with the positive y-direction ($\vec{j}$) and to the zenith with the positive z-direction ($\vec{k}$). With , θ and ϕ, the components in Cartesian coordinates are:

$$\begin{aligned} u_x &= U \cdot \cos\phi \cdot \sin\theta \\ u_y &= U \cdot \cos\phi \cdot \cos\theta \\ u_z &= U \cdot \sin\phi \end{aligned} \tag{B.3}$$

and the three-dimensional wind vector becomes:

$$\vec{u} = \begin{pmatrix} U \cdot \cos\phi \cdot \sin\theta \\ U \cdot \cos\phi \cdot \cos\theta \\ U \cdot \sin\phi \end{pmatrix} \tag{B.4}$$

EXAMPLE Horizontal west wind: $\theta = 90°$, $\varphi = 0°$.

$$\Rightarrow u_x = U, u_y = u_z = 0 \quad \vec{u} = (U,0,0)$$

B.3 Horizontal wind vector

The horizontal wind vector, $\vec{u}_h$, and the horizontal projection of the three-dimensional wind vector, $\vec{u}$, in Figure B.1 becomes:

$$\vec{u}_h = \begin{pmatrix} u_x \\ u_y \end{pmatrix} = \begin{pmatrix} u_h \cdot \sin\theta \\ u_h \cdot \cos\theta \end{pmatrix} \tag{B.5}$$

or, in component notation:

$$u_h = |\vec{u}_h| = U \cdot \cos\phi = \sqrt{u_x^2 + u_y^2} \tag{B.6}$$

The value u_h is denoted as horizontal wind velocity or colloquially as wind velocity. According to the meteorological convention, the wind direction is defined as the direction opposite to the wind vector, $\vec{u}_h$. It is oriented clockwise from North via East, South and West (see Figure B.1).

For the case of a lidar scanning in a disk at fixed elevation angle in uniform wind flow, the individual line-of-sight velocity points follow a cosine form as a function of azimuth angle. The peaks of the function correspond to the azimuth angle aligned parallel or anti-parallel to the wind direction. The function passes through zero when the azimuth angle is perpendicular to wind bearing since there is no component of velocity along the line of sight. The data are also conveniently displayed on a polar plot, which provides information at a glance on the speed, direction and vertical wind component. A standard least-squares fitting routine provides the best estimates of the values of the three unknown parameters (either *u*, *v* and *w*, or alternatively, horizontal speed, vertical speed and wind bearing).

B.4 Radial velocity

In lidar measurements, the component v_r of the local wind vector $\vec{u}(\vec{r},t)$ the beam direction of the laser, i.e. the radial velocity at any arbitrary position $\vec{r}$ is the direct measurand determined from the Doppler frequency shift (see Figure 5). If the wind vector $\vec{u}(\vec{r})$ is written in a spherical coordinate

system ($\vec{e}_r$, $\vec{e}_\theta$, $\vec{e}_\phi$) instead of a Cartesian ($\vec{i}$, $\vec{j}$, $\vec{k}$) coordinate system, the radial velocity, v_r, is easily defined (compare Formula (B.2))[20]:

$$\vec{u}(\vec{r}) = \vec{u}(r,\theta,\phi) = \left(u_r \cdot \vec{e}_r + u_\theta \cdot \vec{e}_\theta + u_\phi \cdot \vec{e}_\phi\right) \tag{B.7}$$

where

$\vec{e}_r$ the unit vector in beam direction;

$\vec{e}_\theta$, $\vec{e}_\phi$ e the unit vectors in the azimuth and elevation direction;

u_r, u_θ, u_ϕ are the orthogonal wind vector components of the coordinate system carried along during the scanning operation.

The projection of the wind vector $\vec{u}(\vec{r})$ onto the beam direction, i.e. the scalar product (∘) can be derived with Formula (B.7):

$$\vec{u}(\vec{r}) \circ \vec{e}_r = u_r \equiv v_r \equiv -v_{LOS} \tag{B.8}$$

v_{LOS} is equal by convention to the negative radial component v_r of the local wind vector at the position $\vec{r}$. The negative sign of v_{LOS} corresponds to the convention that in lidar systems the wind velocity is regarded as positive towards the laser.

With the known transformation relation between spherical and Cartesian coordinates[19], v_r can be expressed by the Cartesian wind components u_x, u_y, u_z the result being:

$$v_{LOS} = -v_r = -\left(u_x \cdot \cos\phi \cdot \sin\theta + u_y \cdot \cos\phi \cdot \cos\theta + u_z \cdot \sin\phi\right) \tag{B.9}$$

B.5 Retrieval of the wind vector

The atmosphere should be sensed at different angles in order to detect the (Cartesian) components u_x, u_y, u_z of the wind vector with the Doppler wind lidar.

NOTE The wind components u_x, u_y, u_z are frequently also called u, v, w.

However, all wind components are usually subject to spatial and temporal fluctuations since the wind field in general cannot be regarded as homogeneous and stationary due to a variety of small scale atmospheric processes like gravity waves, convection, turbulence or orographically induced flow effects. Homogeneity assumptions should therefore be made in order to retrieve an estimate of the wind vector from the radial components. The better this assumption holds, the more does the estimate represent the actual wind field. The problem has been extensively discussed in the literature and is explained in textbooks for both radar and lidar, see, for example, References [21] and [22].

Therefore, assuring that the wind field can be regarded as stationary over the measurement period and horizontally homogeneous over the sampled volume, that is, if the wind field is only a function of the vertical coordinate z, then the radial wind measurements for a fixed geometrical height are given by Formula (B.10), the simple matrix equation:

$$A \cdot u = v_r \tag{B.10}$$

The rows of this (n x 3) matrix A are comprised of the unit directional vectors describing the pointing of the n beams. The vector v_r is also of dimension n and contains the radial winds obtained in the n pointing directions. This is nothing more than a compact notation for the n scalar (inner) products as

given in Formula (B.8). For $n = 3$, the inverse A^{-1} exists if A has rank 3 (e.g. all row vectors are linearly independent) and the wind vector can be directly obtained through Formula (B.11):

$$u = A^{-1} \cdot v_r \tag{B.11}$$

For $n > 3$ and rank(A) = 3, the linear system is overdetermined and has usually either one solution or no (exact solution) at all. However, an approximate solution can be found which minimizes $\left\| A \cdot u - v_r \right\|^2$. This least-square solution can be expressed by the Pseudoinverse $(A^T A)^{-1} \cdot A^T$ of matrix A as shown in Formula (B.12):

$$u = (A^T A)^{-1} \cdot A^T \cdot v_r \tag{B.12}$$

A^T denotes the transpose of matrix A. Formula (B.12) is sufficiently general and describes all possible scanning configurations with n discrete beam pointing directions. Care shall be taken in the practical use of this formula to obtain numerically stable implementations.

The Doppler beam swinging (DBS) technique or the velocity azimuth display (VAD) scanning methods are two frequently used scan schemes for Doppler lidars.

In the case of the DBS technique, measurements are performed in at least three linearly independent directions. This method allows for a very fast scanning, but it may yield biased measurements if the wind field is non-homogeneous. The validity of the retrieval assumptions (homogeneity, stationarity) can be tested to some extend if more than three directions are used. An explicit example of the DBS method with $n = 3$ and $n = 4$ can be found in Reference [23].

In the case of the VAD scan, the beam direction azimuth is varied in a continuous scanning operation. The variation of the azimuth angle during the measurement series yields a set of different projections of the local wind vector onto these measurement directions. The elevation angle remains constant in the process. Originally, the VAD method was proposed for a horizontally homogeneous wind field[24], later discussions were extended to allow for an additional linear variation of the vector components[25]. In the case of a homogeneous wind field, the result is a sinusoidal profile of the measured velocity v_{LOS}.

If the lidar is powerful enough to provide several azimuth scans at different elevations in reasonable time, these can be combined in order to compile a full volume scan. This makes it feasible to use a more elaborate model of the wind field that can be fitted to the vector of observations of v_r. That is, analogous to Formula (B.10), one can further expand the Taylor series incorporating also shearing of the wind, i.e. the first spatial derivatives. For Doppler radars, this procedure is standard and is commonly known as volume velocity processing (VVP). It has been originally published in Reference [26]. This analysis then leads to Formula (B.13) instead of Formula (B.10):

$$\begin{aligned} v_r &= \sin\theta \cdot \cos\phi \cdot u_0 + \cos\theta \cdot \cos\phi \cdot v_0 + \sin\phi \cdot w_0 \\ &+ r \cdot \sin^2\theta \cdot \cos^2\phi \cdot u'_x \\ &+ r \cdot \cos^2\theta \cdot \cos^2\phi \cdot v'_y \\ &+ r \cdot \cos\theta \cdot \sin\theta \cdot \cos^2\phi \cdot \left(u'_y + v'_x\right) \\ &+ \sin\phi \cdot \left(r \cdot \sin\phi - z_0\right) \cdot w'_z \\ &+ \sin\theta \cdot \cos\phi \cdot \left(r \cdot \sin\phi - z_0\right) \cdot \left(u'_z + w'_x\right) \end{aligned} \tag{B.13}$$